



CHAPTER IV

RESULTS AND DISCUSSION

4.1 Catalyst Characterization

In this study, the synthesized HZSM-5 catalysts, which used NaOH as a mineralizing agent, ($\text{SiO}_2/\text{Al}_2\text{O}_3$ ratio of ca. 195) obtained at 120 °C for crystallization 48, 72, and 96 h are designated as HZ5-A1(w), HZ5-A2(w), and HZ5-A3(w), respectively, and those obtained at 140 °C for 48, 72, and 96 h are designated as HZ5-B1(w), HZ5-B2(w), and HZ5-B3(w), respectively, where w is the molar ratio of the $\text{H}_2\text{O}/\text{SiO}_2$ in the initial gel.

In the first period of this work, HZSM-5 catalyst synthesized by another mineralizing agent had been studied also, NH_4F as a mineralizing agent was chosen. The synthesized HZSM-5 catalysts, which used NH_4F as a mineralizing agent obtained at 120 °C for 72 h is designated as HZ5-F1(w), obtained at 140 °C for 72 h is designated as HZ5-F2(w), and obtained at 170 °C for 42 h is designated HZ5-F3(w). The catalyst procedure is presented in flow diagram as seen in Figure 4.1.

However, HZSM-5 catalysts synthesized by NH_4F were observed later that $\text{SiO}_2/\text{Al}_2\text{O}_3$ molar ratios clearly fluctuated and missed the target value of $\text{SiO}_2/\text{Al}_2\text{O}_3$ molar ratios of 195, rather much higher than the target value. Therefore, in this chapter, HZSM-5 catalysts synthesized by NH_4F utilization were not suitable to discussed and/or compared the catalyst characterization and the catalytic activity testing with themselves and/or the another group of catalysts synthesized NaOH utilization. Anywise, some parts of the catalyst characterizations and the mimetic catalytic activity results of HZSM-5 catalysts synthesized by NH_4F utilization was insulated in the appendix section.

4.1.1 X-ray Diffraction

Figure 4.2 shows the XRD patterns of some synthesized HZSM-5 zeolites. The findings reveal that all the patterns of samples are characteristics of MFI. The characteristic diffraction peak intensity is substantially pronounced implying that all the materials have a high crystallinity.

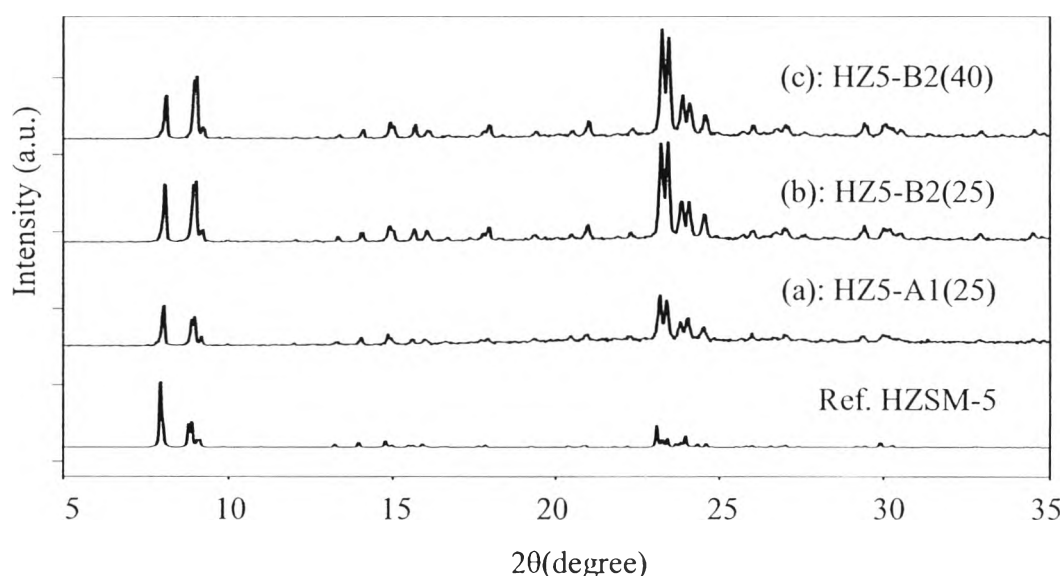


Figure 4.2 X-ray diffraction patterns of the synthesized HZSM-5.

The intensity peaks at 2θ of 7.94, 8.88, 13.96, 14.78, 20.90, 23.08, 23.24, 23.40, 23.96, 24.58, and 25.84° are ascribed to an HZSM-5 zeolite (www.iza-structure.org/database/). Figures 4.2(a) and 4.2(b) indicate XRD patterns of samples synthesized with changing crystallization temperature and time from 120°C , 48 h to 140°C , 72 h. The peak intensity of the as-synthesized HZSM-5, at high synthesis temperature and time (140°C , 72 h) is higher than that of the HZSM-5 synthesized at low synthesis temperature and time (120°C , 48 h). Figure 4.2(c) indicates the XRD pattern of the sample synthesized at elevated temperature with increased $\text{H}_2\text{O}/\text{SiO}_2$ ratio from 25 to 40. The peak intensity at $7.94(20)$ of HZ5-B2(25) possesses slightly higher than that of HZ5-B2(40). It implied that less amount of water content, viscosity of the aluminosilicate gel would be suitably dense for substrates to diffuse

freely and/or interact to each other, leading to achieve formation of ZSM-5, which resulted in high peak intensity (Gu *et al.*, 2009).

4.1.2 Scanning Electron Microscopy (SEM)

Morphological properties and crystal sizes of the product samples were investigated by SEM. The results are presented in Figure 4.3 and Table 4.1. Figure 4.3 shows the SEM images of HZSM-5; (a) HZ5-A1(25), (b) HZ5-A2(25), (c) HZ5-A3(25), (d) HZ5-B1(25), (e) HZ5-B2(25), (f) HZ5-B3(25), and (g) HZ5-B2(40). It can be found that the HZSM-5 synthesized by NaOH is consistent with the character of micro scale crystal.

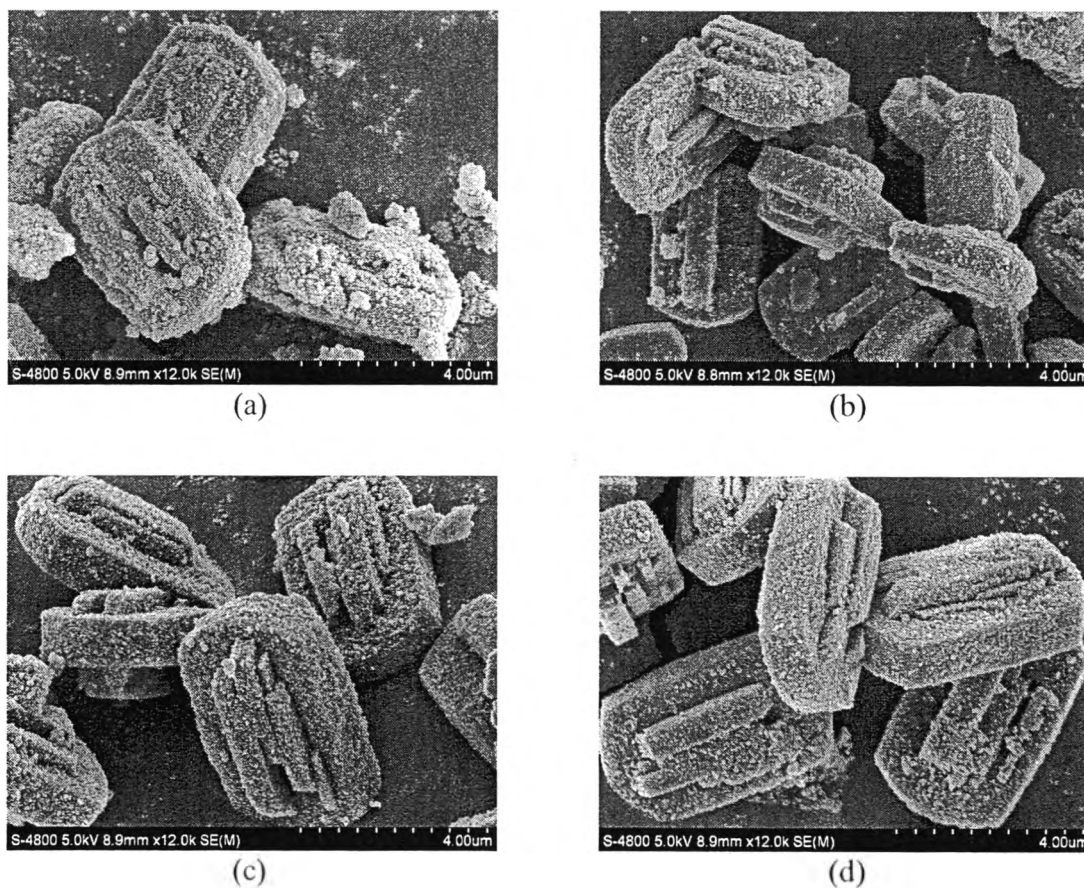


Figure 4.3 The SEM images of HZSM-5 catalysts (a) HZ5-A1(25), (b) HZ5-A2(25), (c) HZ5-A3(25), and (d) HZ5-B1(25).

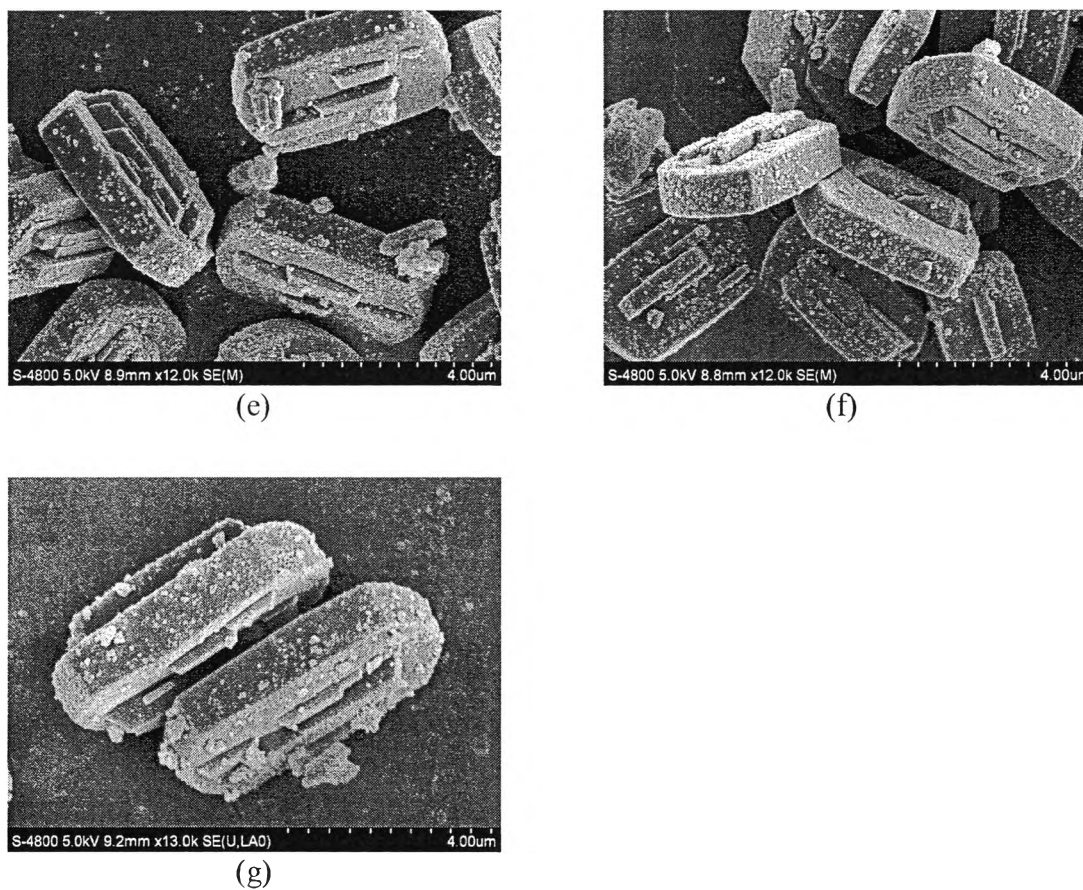


Figure 4.3 (cont'd) The SEM images of HZSM-5 catalysts (e) HZ5-B2(25), (f) HZ5-B3(25), and (g) HZ5-B2(40).

Table 4.1 Crystal sizes of the synthesized HZSM-5 catalysts

Catalyst	Dimension (WxLxH, micron)
(a) HZ5-A1(25)	3.1 x 4.5 x 1.2
(b) HZ5-A2(25)	2.3 x 3.5 x 1.0
(c) HZ5-A3(25)	3.3 x 5.1 x 1.2
(d) HZ5-B1(25)	3.2 x 5.2 x 1.2
(e) HZ5-B2(25)	2.9 x 4.8 x 1.1
(f) HZ5-B3(25)	3.1 x 5.2 x 1.3
(g) HZ5-B2(40)	4.5 x 6.3 x 1.5

It is noticed that the different mineralizing agents and different synthesis conditions can provide different types of morphology. Figures. 4.3(a) - 4.3 (g) show the SEM images of the HZSM-5 synthesized by NaOH utilization, the morphologies of those were irregular hexagonal prisms with rectangular insertion with crystal sizes of 3.5–6.3 μm in length, about 2.3-4.5 μm in width, and a narrow range of 1.0-1.5 μm in height. Although, at low temperature and/or time of synthesis still have many clusters of smaller crystals like a spherical crystal. Normally, short synthesis time and low synthesis temperature could provide smaller crystal size (Khatamian *et al.*, 2009), but HZ5-A1(25) synthesized at the lowest time and temperature did not provide an expected crystal size as the smallest crystal size, which may be due to its larger aggregated crystal cluster.

From Table 4.1, the crystal sizes were not ordered respectively with the synthesis time, as Khatamian *et al.* (2009) mentioned. However, the synthesis temperature was significant to the crystal size. For $\text{H}_2\text{O}/\text{SiO}_2$ ratio of 25, it was noticed that the crystal size of the HZSM-5 synthesized at same synthesis time increased with increasing the synthesis temperature from 120 $^\circ\text{C}$ to 140 $^\circ\text{C}$. Anywise, it was clearly observed that the crystal size was the smallest at 72 h of synthesis time, followed by 48 h and 96 h, respectively, for both cases of synthesis temperature.

When consider the variation of $\text{H}_2\text{O}/\text{SiO}_2$ ratio in the initial gel of the catalyst (HZ5-B2(25) and HZ5-B2(40)) from 25 to 40, it was indicated that the crystal size was decreased with a decrease in the molar composition of water. According to Suzuki *et al.* (1987), the low ratios of $\text{H}_2\text{O}/\text{SiO}_2$, the short distance between nutrients in the aqueous solution should have enhanced the nucleation and thus crystallization resulted in smaller crystal size.

4.1.3 Surface Area Measurements

The textural properties of the synthesized catalysts determined by N_2 adsorption-desorption method are shown in Table 4.2. The BET surface areas were insignificantly varied for all of the catalysts, ranging from 314 to 390 m^2/g . In the case of NaOH utilization, the micropore volume tend to significantly increase with increasing synthesis temperature and time, because the growth rate of zeolite crystallization at high temperature is faster than that of lower temperature, as a result

in increment of micropore volume. However, the variation of H_2O/SiO_2 ratio in the initial gel of the catalyst (HZ5-B2(25) and HZ5-B2(40)) from 25 to 40 resulted in higher micropore volume which had been obtained with increasing the amount of water content in the initial gel. The total pore volume has grew in the opposite way to the micropore volume, it seems to significantly decrease with increasing synthesis temperature and time, the total pore volume is considerably decreased with increasing temperature and time. Since, under hydrothermal synthesis, water, which is used to stabilize the porous products by filling the pores, vastly evaporates out of the pore at high temperature, as a result, the denser phases will become higher. Hence, the amount of porous structure will decrease (Ertl *et al.*, 2008).

The micropore to total pore volume (Mi/T) ratio was introduced as a parameter to be related to the catalyst activity. It is beneficial to compensate the fluctuation of the total pore volume.

Table 4.2 Textural properties of the synthesized HZSM-5 catalysts

Catalyst	BET	Micropore	Total Pore	Mi/T ratio
	Surface Area (m ² /g)	Volume(Mi) ^a (cm ³ /g)	Volume(T) (cm ³ /g)	
HZ5-A1(25)	314	0.059	0.447	0.132
HZ5-A2(25)	352	0.114	0.334	0.341
HZ5-A3(25)	329	0.122	0.270	0.452
HZ5-B1(25)	358	0.146	0.248	0.589
HZ5-B2(25)	337	0.138	0.233	0.592
HZ5-B3(25)	366	0.157	0.226	0.695
HZ5-B2(40)	345	0.151	0.193	0.782

^a Determined by t method

4.1.4 Catalyst Composition

The chemical compositions of synthesized HZSM-5 catalysts are analyzed by X-ray fluorescence (XRF) technique. The results are summarized in Table 4.3. From the data, the Si/Al and/or SiO₂/Al₂O₃ molar ratios are determined. It was found that HZSM-5 catalysts synthesized by NaOH utilization provide SiO₂/Al₂O₃ molar ratios in the range of 176 to 227, it is notice that the effect of synthesized time and temperature to the catalyst composition are not significant for the case of NaOH utilization.

Table 4.3 The chemical compositions of synthesized HZSM-5 catalysts

Catalyst	Compound (mol %)			Si/Al	SiO ₂ /Al ₂ O ₃
	Si	Al	Na		
HZ5-A1(25)	98.848	0.986	0.166	100.2	200
HZ5-A2(25)	98.585	1.118	0.297	88.2	176
HZ5-A3(25)	98.883	0.871	0.247	113.6	227
HZ5-B1(25)	98.890	0.926	0.184	106.8	214
HZ5-B2(25)	98.777	0.980	0.243	100.8	202
HZ5-B3(25)	98.843	1.009	0.148	97.9	196
HZ5-B2(40)	98.953	0.954	0.093	103.7	207

4.1.5 Acidity Determination

The Brönsted acid site of HZSM-5 catalysts was quantitatively and qualitatively determined by the TPD of adsorbed isopropylamine (TPD-IPA). The theoretical acidity was determined based on the number of protons attained according to its formula. Lewis acid site is the result in difference between the theoretical acidity and the Brönsted acid site. The quantitative values of acidity for the catalysts are shown in Table 4.4. From Table 4.4, it was found that the Brönsted acid sites tend to rather increase with increasing the crystallization temperature and time.

The B/L ratio is the Brönsted acid site to the Lewis acid site ratio. The B/L ratio at 120 °C tend to increase with increasing the synthesis time. However, at 140 °C, the B/L ratio is likely to increase with increasing the synthesis time, excepted for HZ5-B3(25), as the B/L ratio is dropped down to 0.242. The new

parameter of TA/(B/L) was introduced as a new parameter to be related to the catalyst activity. It was obvious that HZ5-A3(25) and HZ5-B2(25) showed somewhat high TA/(B/L).

Figures 4.4(a) – 4.4(c) show the relationships between the acidity properties and synthesis conditions with water to silica ratio (H_2O/SiO_2) of 25. Figure 4.4(a) clearly indicates that the Brönsted acid site tends to increase with increasing synthesis temperature and time. Similar to the first one, the tendency of the B/L ratio against synthesis conditions, Figure 4.4(b), is increased with increasing synthesis temperature and time also. On the other hand, TA/(B/L), Figure 4.4(c), is it decreased with increasing synthesis temperature and time, it is probably due to the increment of the B/L ratio at high synthesis temperature and long synthesis time. However, Figures 4.4(d) indicates that the B/L ratio depends on both of the Brönsted acid site and theoretical acidity, as for low theoretical acidity resulting in low amount of Lewis acid site ratio, thus leading to a high B/L ratio.

Table 4.4 The quantitative values of acidity for the HZSM-5 catalysts

Catalyst	Brönsted acid site (mmol/g)	Theoretical Acidity (TA) (mmol/g)	Lewis acid site (mmol/g)	B/L ratio	TA / (B/L) (mmol/g)
HZ5-A1(25)	0.0208	0.136	0.115	0.181	0.75
HZ5-A2(25)	0.0266	0.135	0.108	0.245	0.55
HZ5-A3(25)	0.0268	0.102	0.076	0.354	0.29
HZ5-B1(25)	0.0238	0.122	0.099	0.242	0.50
HZ5-B2(25)	0.029	0.121	0.092	0.314	0.39
HZ5-B3(25)	0.0278	0.143	0.115	0.242	0.59
HZ5-B2(40)	0.0242	0.143	0.119	0.204	0.70

* The theoretical acidity was determined based on the number of protons is attained according to its formula, which used catalyst composition from X-ray fluorescence (XRF) technique

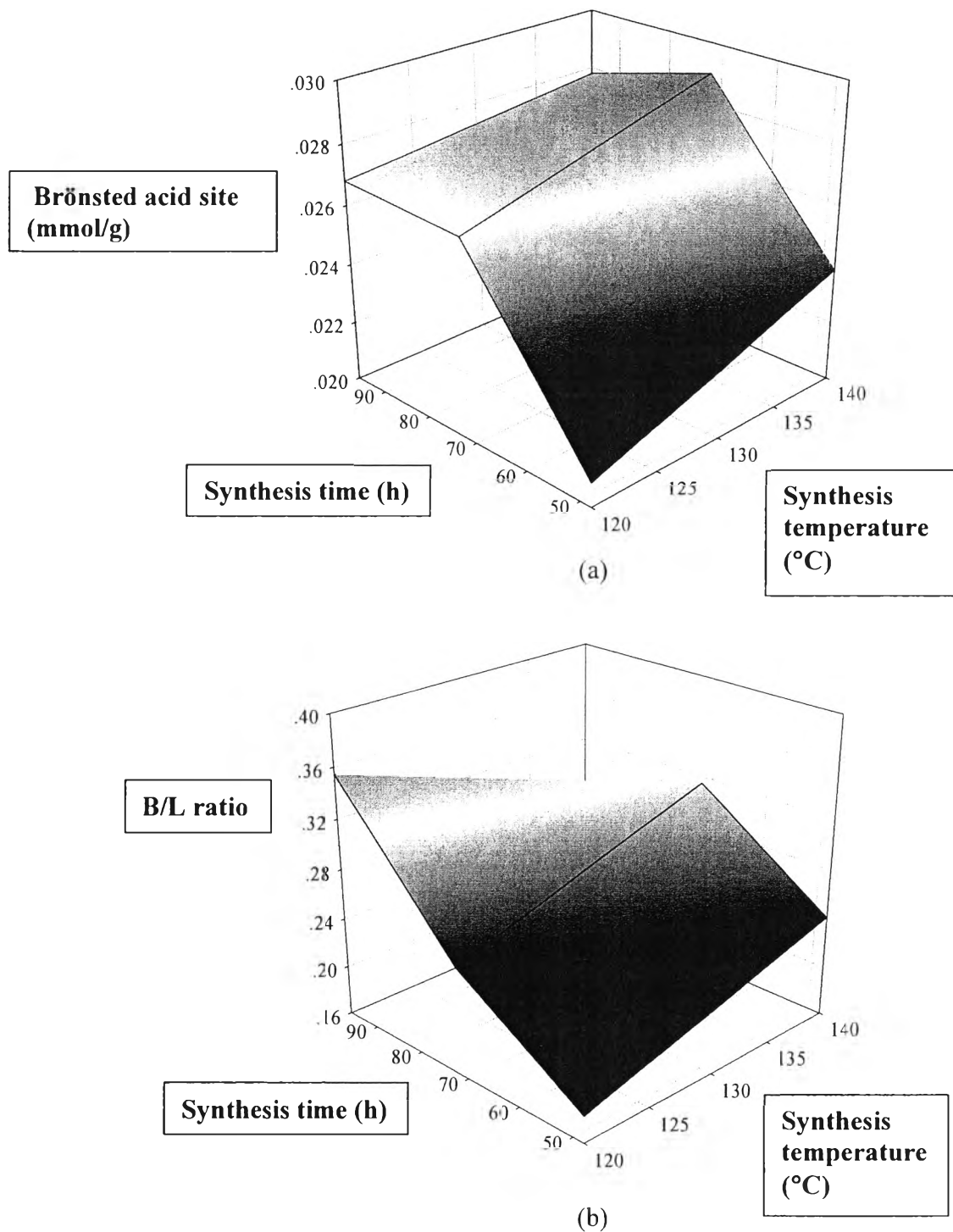
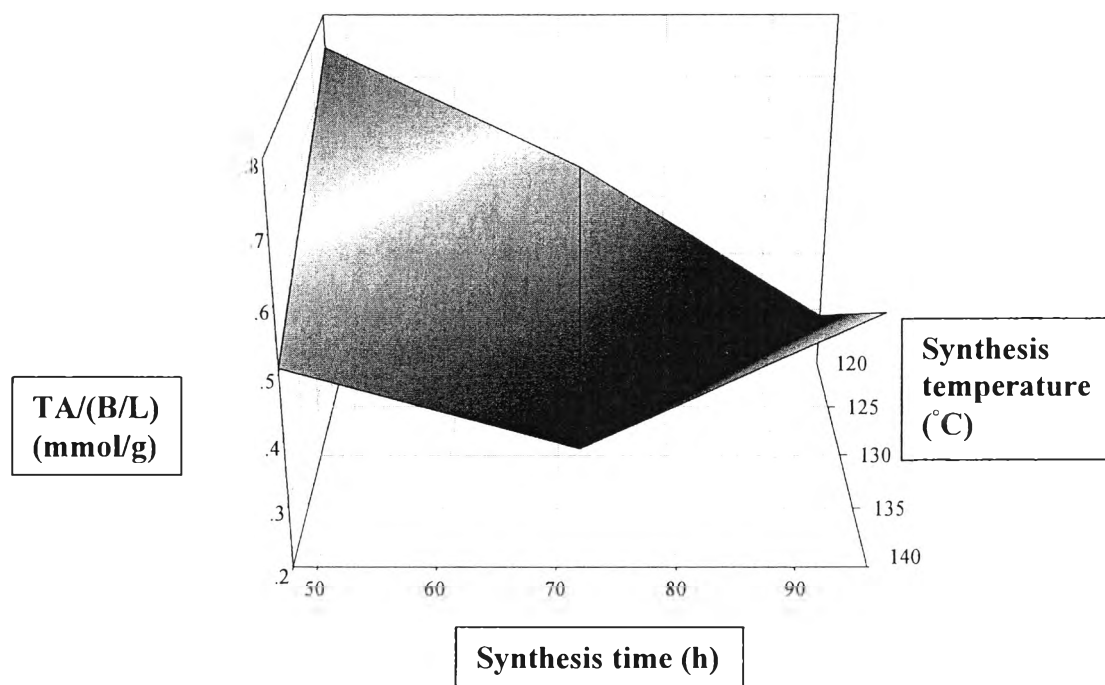
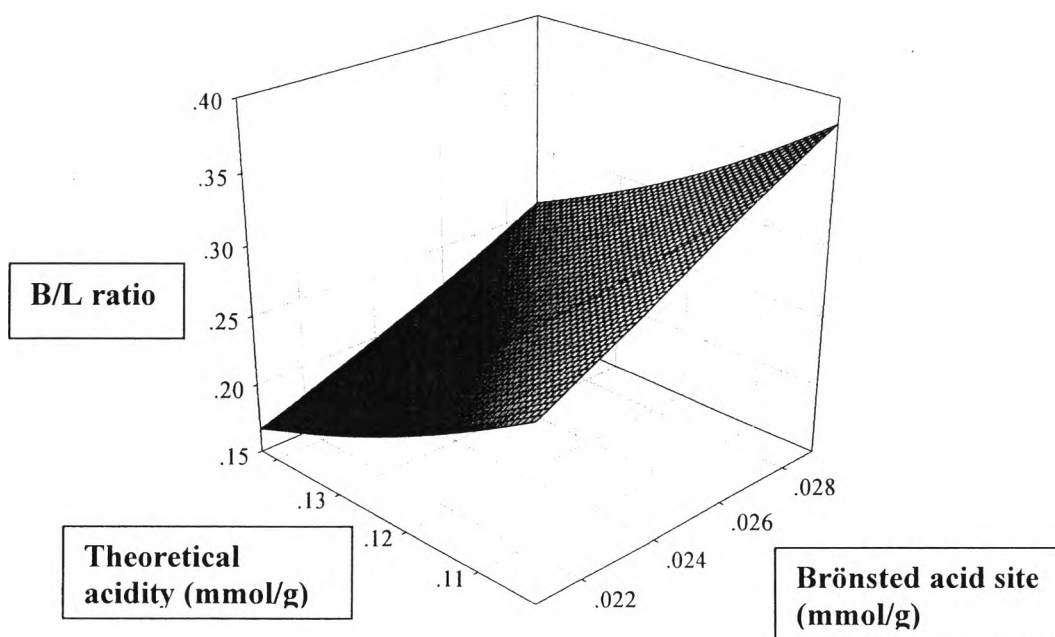


Figure 4.4 The plots of acidity variation as functions of synthesis conditions : (a) Synthesis temperature and time vs Brønsted acid site, (b) Synthesis temperature and time vs B/L ratio.



(c)



(d)

Figure 4.4 (cont'd) (c) Synthesis temperature and time vs TA/(B/L), (d) Theoretical acidity and Brönsted acid site vs B/L ratio.

4.2 Catalytic Activity Testing

The catalytic activity of the catalysts is tested in a fixed-bed continuous down-flow reactor under the reaction conditions as follows: temperature (300 °C to 600 °C), morphology of catalysts, benzene-to-ethanol ratio (1 to 4), and weight hourly space velocity (10-20 h⁻¹). The results of catalytic performance of alkylation of benzene with ethanol are carefully investigated.

4.2.1 Effects of Textural Properties and Acidity

Table 4.5 shows the catalytic activity of the synthesized HZSM-5 catalysts on the alkylation of benzene with ethanol at T = 500 °C, the feed ratio 4:1 for benzene:ethanol, WHSV = 20 h⁻¹, and TOS = 410 min. For the catalytic activity, it could not conclude mutually between HZSM-5 synthesized by NaOH utilization and HZSM-5 synthesized by NH₄F utilization, as mentioned previously, SiO₂/Al₂O₃ of HZSM-5 synthesized by NH₄F utilization has not approach to the target of 195, so it should not be investigated the catalytic activity together with NaOH utilization. For the case of NaOH utilization, the HZ5-A2(25) provided the highest EB selectivity HZ5-A2(25) observed to be the smallest crystal size than the other. If the crystal was too large as seen in HZ5-B2(40), ethylbenzene did not diffuse from the pore quickly, so the secondary reactions increased resulted in the lowest EB selectivity. Hence, the small crystal is beneficial for ethylbenzene diffusion and increases high ethylbenzene selectivity (Gao *et al.*, 2010).

Table 4.2 indicates that HZ5-A2(25) was almost lowest Mi/T ratio indicating the dominance of mesopore volume. The plentiful of micropore would allow EB to diffuse out of the pore more difficult than the other having the abundance of mesopores. Moreover, the dominance of mesopore volume is inescapably related to the contact time, which the increment of the contact time between the rest of ethylbenzene in the pore and other carbenium ion can be negative effect to the product quality in terms of EB selectivity. A consequence of the narrow pore volume can provide the contact time between ethylbenzene and carbenium ion, so ethylbenzenes were easy to crack or form to the other undesirable products.

However, the HZ5-A1(25) has the higher amount of mesopore volume than HZ5-A2(25), but its EB selectivity was lower than HZ5-A2(25), which may be due to its larger aggregated crystal cluster, larger crystal size, and/or improper the amount of acid site than HZ5-A2(25). On the contrary, benzene conversion tends to increase with increasing Mi/T ratio, it can be attributed that the increase of micropore volume may allow any products and/or benzene to diffuse out of the pores difficultly, so the benzene remaining in the pore can have enough time to react with anything in the pore, which that resulted in high benzene conversion. However, the acid site on catalyst surface may affect benzene conversion also, as seen in HZ5-A3(25) and HZ5-B2(25) which have the highest and almost highest B/L ratio, respectively, which that may provide secondary reactions and bulky molecules as it may block active site.

It is well known that acidity plays an important role in alkylation reactions. A strong acid site is beneficial for secondary reactions such as decomposition, isomerization, and polymerization (Zhu *et al.*, 2006, 2007). In this work, the parameter of TA/(B/L) was introduced as a new parameter to be related to the catalyst activity. From Figure 4.6, the HZ5-A2(25), A2, was chosen as an intermediate point, it clearly shows that on the left hand side of the intermediate point, the EB selectivity tended to increase with increasing TA/(B/L), the effect of low the TA/(B/L) was probably because of too high B/L ratio. As mentioned above, if the B/L ratio was too high, the secondary reactions and bulky molecules were easier to formed, which that may resulted in low EB selectivity and benzene conversion in HZ5-A3(25) and HZ5-B2(25). On the right hand side of the intermediate point, when consider the of effect of acidity to HZ5-A1(25), it was observed that EB selectivity tends to decrease with increasing TA/(B/L), it implied that too high TA/(B/L) can result in low EB selectivity also, howsoever, the effect of high the TA/(B/L) for this case was probably because of too low B/L ratio, the storage of the active site on catalyst surface may resulted in low EB selectivity also. In addition, the optimal TA/(B/L) of 0.55 was observed to provide the highest ethylbenzene selectivity around 94.91 %, followed by HZ5-B3(25) halving TA/(B/L) of 0.59 as close to that of HZ5-A2(25).

Table 4.5 The catalytic activity and surface properties characterization of the synthesized HZSM-5 at T = 500 °C, B/E = 4, WHSV = 20 h⁻¹, and TOS = 410 min

Catalyst	EB Selectivity (%)	Benzene Conversion (%)	Mi/T ratio	Theoretical Acidity(TA) (mmol/g)	TA / (B/L) (mmol/g)
HZ5-A1(25)	94.56	5.79	0.132	0.136	0.75
HZ5-A2(25)	94.91	7.50	0.341	0.135	0.55
HZ5-A3(25)	94.55	3.00	0.452	0.102	0.29
HZ5-B1(25)	94.63	8.33	0.589	0.122	0.50
HZ5-B2(25)	94.62	3.28	0.592	0.121	0.39
HZ5-B3(25)	94.78	8.78	0.695	0.143	0.59
HZ5-B2(40)	94.30	9.21	0.782	0.143	0.70

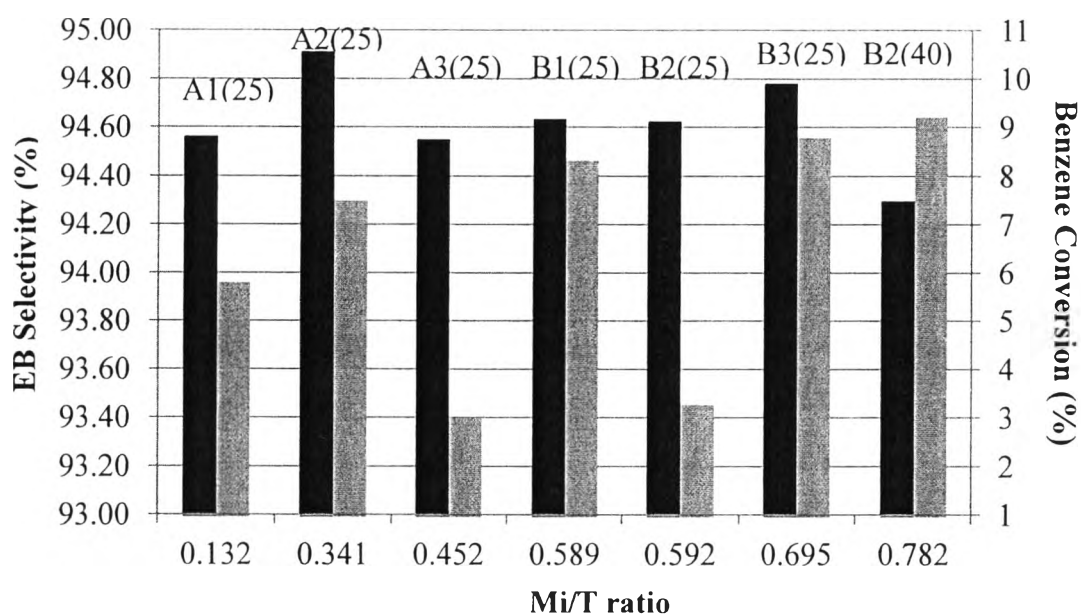


Figure 4.5 The plots of Mi/T ratio vs EB Selectivity and benzene conversion ((■) EB selectivity, and (■) benzene conversion) at T= 500 °C, B/E = 4, WHSV = 20 h⁻¹, and TOS = 410 min.

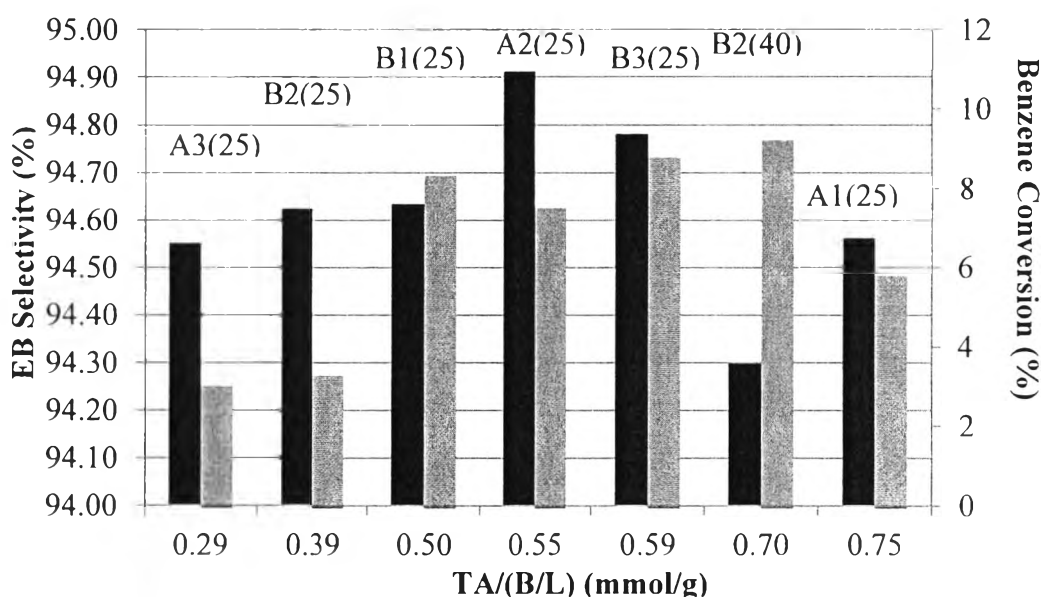


Figure 4.6 Graph plotted between TA/(B/L) vs EB Selectivity and benzene conversion ((■) EB selectivity, and (■) benzene conversion) at $T = 500\text{ }^{\circ}\text{C}$, $B/E = 4$, $WHSV = 20\text{ h}^{-1}$, and $TOS = 410\text{ min}$.

From above section which demonstrates that HZ5-A2(25) was the best catalyst providing suitable Mi/T ratio, crystal size, and surface acid properties as well as catalytic activity in terms of EB selectivity. Therefore, the HZ5-A2(25) was brought to perform the ethylation of benzene with ethanol to optimize reaction conditions such as reaction temperature, B/E feed molar ratio, WHSV, and to determine its coke formation.

4.2.2 Effect of Reaction Temperature

The catalyst was studied at 300, 400, 500 and 600 $^{\circ}\text{C}$ over HZ5-A2(25), with the feed ratio 4:1 for benzene:ethanol, $WHSV = 20\text{ h}^{-1}$, and $TOS = 410\text{ min}$. The plots of benzene conversion, ethanol conversion, and EB selectivity versus temperature for HZ5-A2(25) catalyst are shown in Figure 4.7. The products of the reaction were found to be EB, diethylbenzenes (DEBs), and polyalkylbenzenes. It shows that the highest EB selectivity is attained at 500 $^{\circ}\text{C}$, ethanol conversions are almost 100% in the investigated temperature range. From the results, it indicates that the optimum temperature providing the highest benzene conversion is 400 $^{\circ}\text{C}$.

According to Gao and co-workers (2010) suggesting about the proper reaction temperature which could not be too low or too high, the decrease in reaction temperature could provide the diffusing out from the pore more slowly affecting the resultant product such as ethylbenzene which would be attacked by a free ethanol or carbenium ion of ethanol, producing DEBs. However, the increase in reaction temperature resulted in the increase in decomposition rate of products, as the decomposition leads to the increase of benzene and bulkier molecules, which block the micropore channels of the catalyst and deactivate the catalyst, corresponding to the result at 600 °C, the decomposition rate resulted in the lowest benzene conversion and EB selectivity.

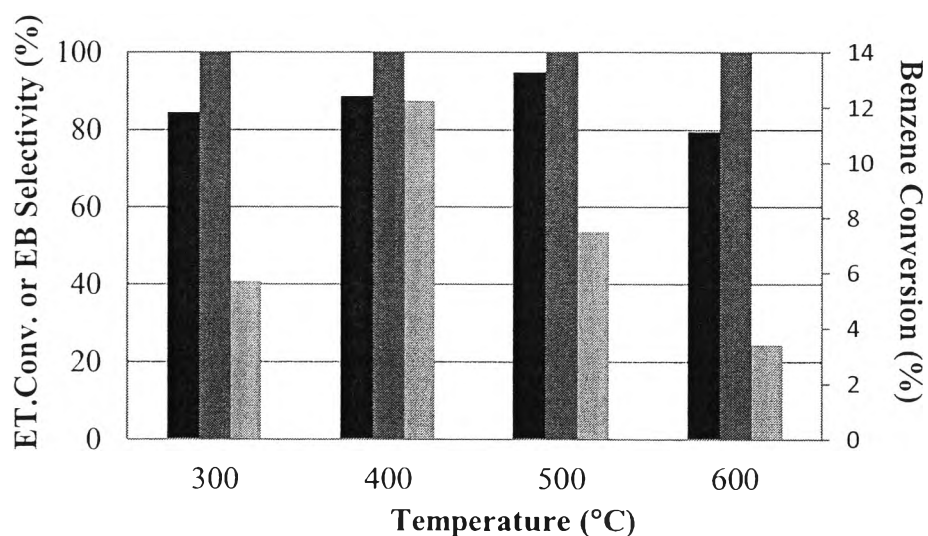


Figure 4.7 Effect of reaction temperature: on (■) EB selectivity, (■) ethanol conversion, and (■) benzene conversion for HZ5-A2(25), B/E = 4, WHSV = 20 h⁻¹, and TOS = 410 min.

Table 4.6 Effect of temperature on the products selectivity over HZ5-A2(25)^a

Temperature (°C)	Selectivity (%)					
	EB	Ethylene	Toluene	Xylenes	DEBs	Others ^b
300	84.60	0.17	0.37	0.33	10.42	4.11
400	88.77	0.06	0.15	0.36	10.12	0.54
500	94.91	0.16	0.24	1.39	2.45	0.85
600	79.58	0.24	2.28	12.38	0.58	4.94

^a Reaction conditions: B/E = 4, WHSV = 20 h⁻¹, time on stream = 410 minute.

^b For example, ethyl toluene, propyl benzene, indane, and naphthalene.

Table 4.6 shows the variation of the reaction products. Normally, at low reaction temperature the polymerization reaction, exothermic reaction, was found to be a main reaction which EB transform itself to be DEBs group. At high reaction temperature the isomerization or cracking reaction, the endothermic reaction, was found to be a main reaction which EB was cracked into Xylenes form. This table shows the products selectivity at different temperatures over HZ5-A2(25). It can be observed that 300 °C and 400 °C behaved the exothermic reaction due to DEBs was shown as a major product of secondary reaction, with a selectivity around 10 %. At 600 °C, its reaction behaved the endothermic reaction because Xylenes was shown as a major product of secondary reaction, with a selectivity around 12 %. However, the reaction was perform at 500 °C provided the highest selectivity to EB (94.91 %), which may be due to not too low or too high reaction temperature as accommodate to form the secondary reaction.

Figure 4.8 represents the products selectivity at different temperature over HZ5-A2(25). When the mass ratios of EB-to-Xylenes and EB-to-DEBs are compared at different temperatures, the optimum highest EB-to-DEBs is obtained at 500 °C with a moderate EB-to-Xylenes ratio. This is because of the exothermic reaction of the alkylation of EB-to-DEBs and the endothermic reaction of the isomerization of EB-to-Xylenes (Ertl G., 2008).

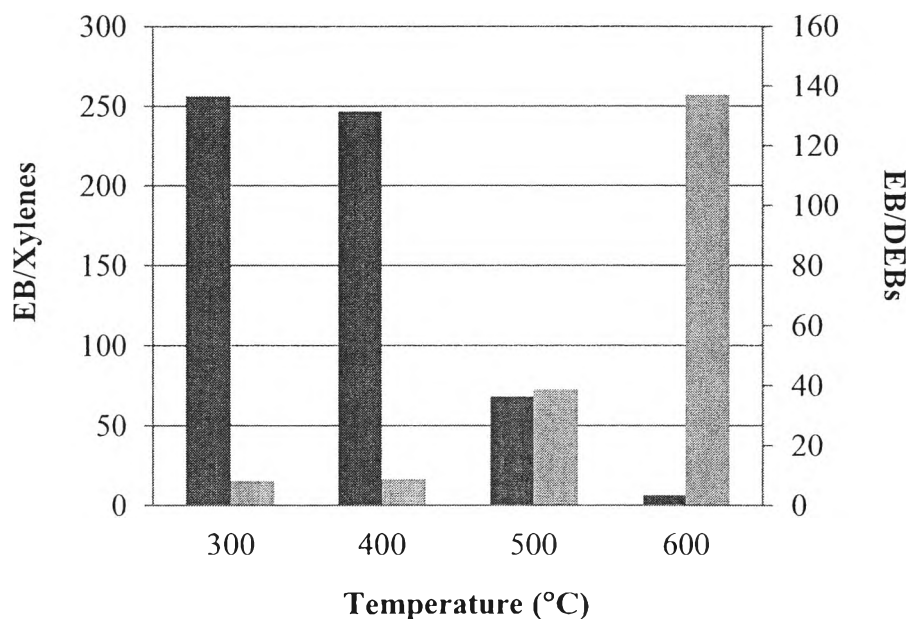


Figure 4.8 Effect of reaction temperature: on (■) EB/Xylenes and (□) EB/DEBs ratios for HZ5-A2(25), B/E = 4, WHSV = 20 h⁻¹, and TOS = 410 min.

4.2.3 Effect of B/E Feed Molar Ratio

The effect of feed molar ratio (benzene to ethanol) on benzene conversion and product selectivity was investigated over HZ5-A2(25) catalyst. Effect of benzene to ethanol mole ratio in the feed mixture on benzene conversion was studied by varying the ratio from 1:1 to 4:1 at 500 °C, and WHSV 20 h⁻¹. Figure 4.9 presents the results of benzene and ethanol conversions as a function of B/E feed molar ratio. The conversion of benzene displays a significant decline with increasing B/E feed ratio from 1:1 to 4:1. This is probably because the increment of B/E feed ratio seem to add a large excess of aromatic reactant to the system which it can interfere the opportunity of benzene interacting with ethyl cations, a large excess of aromatic reactant can block the rest of the active sites of the catalyst surface (Odedairo *et al.*, 2010), as a lower benzene conversion is obtained. However, the ethanol conversion still keep constant almost 100% conversion at all B/E feed molar ratios.

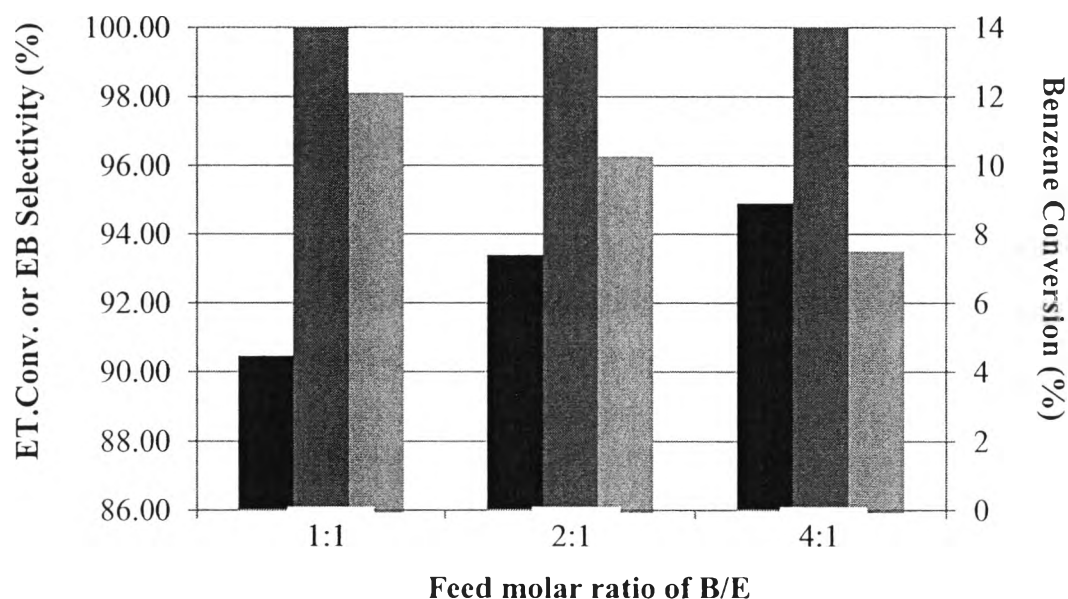


Figure 4.9 Effect of B/E feed ratio: on (■) EB selectivity, (■) ethanol conversion, and (■) benzene conversion for HZ5-A2(25), $T = 500\text{ }^{\circ}\text{C}$, $\text{WHSV} = 20\text{ h}^{-1}$, and $\text{TOS} = 410\text{ min}$.

Table 4.7 Effect of B/E feed molar ratio on the products selectivity over HZ5-A2(25)^a

B:E feed ratio	Selectivity (%)					
	EB	Ethylene	Toluene	Xylenes	DEBs	Others ^b
1:1	90.46	0.10	0.15	0.73	7.66	0.90
2:1	93.40	0.12	0.19	1.00	4.49	0.80
4:1	94.91	0.16	0.24	1.39	2.45	0.85

^a Reaction conditions: $T = 500\text{ }^{\circ}\text{C}$, $\text{WHSV} = 20\text{ h}^{-1}$, time on stream = 410 minute.

^b For examples, ethyl toluene, propyl benzene, indane, and naphthalene.

Table 4.7 shows the effect of B/E feed ratio to the products selectivity. The selectivity to EB increased with increasing B/E feed ratio whereas the selectivity to DEB isomers decreased. This might be also resulted from the dilution of ethanol. The results attainable were conformed to those obtained by Odedairo *et al.* (2010) with which the high EB selectivity at higher benzene to ethanol ratios was attributed to the suppression of further alkylation of EB by ethyl cations.

4.2.4 Effect of WHSV

Figure 4.10 presents the results of ethylbenzene selectivity, benzene conversion, and ethanol conversion against WHSV (weight hourly space velocity). The reaction was investigated over HZ5-A2(25) catalyst at 500 °C with the B/E feed ratio 4:1, and varying WHSV with 10 and 20 h⁻¹. It can be observed that ethanol conversions were constant in both cases of 10 and 20 h⁻¹. However, benzene conversion was significantly decreased with increasing WHSV from 10 to 20 h⁻¹. This can be interpreted in lieu of the contact time. With a decrease in the WHSV, a longer contact time between the active sites of the catalyst surface and feed reactants can lead to higher probability for the secondary reactions to occur consuming more benzene. On the contrary, the increased EB selectivity with increasing WHSV can be attributed to the suppression of secondary reactions caused by reducing the contact time providing the diffusion of the product out from the reaction zone quickly, thus leading to high EB selectivity.

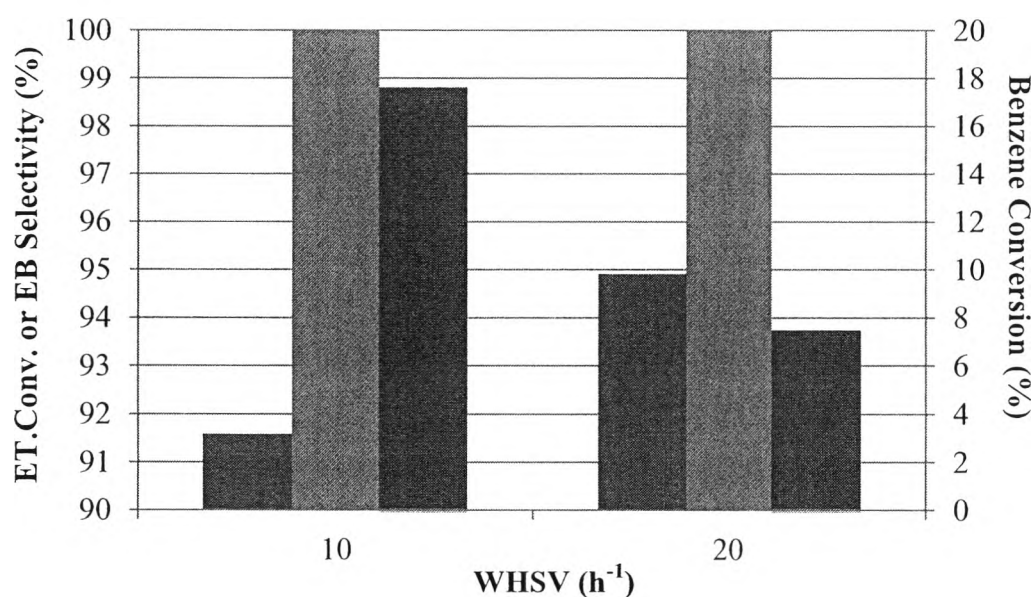


Figure 4.10 Effect of WHSV: on (■) EB selectivity, (■) ethanol conversion, and (■) benzene conversion for HZ5-A2(25), B/E = 4, T = 500 °C, and TOS = 410 min.

4.2.5 Coke Formation

The spent catalysts were analyzed by the temperature programmed oxidation (TPO) technique to observe the coke formation over the HZ5-A2(25) catalysts at different B/E feed molar ratios along with specific reaction conditions: $T = 500\text{ }^{\circ}\text{C}$, $\text{WHSV} = 20\text{ h}^{-1}$, and $\text{TOS} = 410\text{ min}$.

Table 4.8 Coke formation of the spent HZ5-A2(25) catalysts

B/E feed molar ratio	Benzene conversion	Amount of carbon (wt%)
1:1	12.11	2.93
2:1	10.28	3.25
4:1	7.50	3.51

As shown in Table 4.8, the amount of coke deposit over the spent HZ5-A2(25) at B/E ratio 1, 2, and 4 are 2.93 wt%, 3.25 wt%, and 3.51 wt%, respectively. It can be observed that the increasing the amount of benzene in feed influencing to the increment of coke formation corresponding to Duang-udom (2011), the coke formation would increase because the benzene could be cracked easier at higher amount of benzene resulting in increasing the tendency of coke formation. As a result, the conversion of benzene will decrease with the coke formation increase.